
An Investigation on Structural, Morphological and Opto-Electrical Properties of Plasmon assisted SnO₂ Photoanode for Photovoltaic Applications

V. Chandrakala, Neena Bachan, W. Jothi Jeyarani, P. Naveen Kumar, B. Praveen, and J. Merline Shyla*

Department of Physics, Energy Nanotechnology Centre (ENTeC),
Loyola Institute of Frontier Energy (LIFE), Loyola College, Chennai 600 034.

*E-mail: jmshyla@gmail.com

Abstract- In the present investigation, we have attempted the incorporation of Plasmon into SnO₂ nanoparticles to tailor their electrical, optical and structural properties for prospective application as photoanode in DSCCs. Bare and Cu assisted SnO₂ nanoparticles were synthesized via facile sol-gel approach and characterized using X-ray Diffraction (XRD), Field Emission Scanning Electron Microscopy (FESEM), UV-VIS Diffuse Reflectance Spectroscopy (DRS), and Field dependent dark and photoconductivity studies. Both samples confirmed the tetragonal structure of SnO₂. FESEM images of bare and Cu assisted samples evidenced nearly spherical nanoparticles. It was found from UV-VIS Diffuse Reflectance Spectra (DRS) that due to Cu incorporation, the absorbance of SnO₂ has extended to the visible portion of the spectrum due to Surface Plasmon Resonance (SPR) phenomena. Field dependent dark and photoconductivity studies revealed that Cu supported SnO₂ nanoparticles show ~ 36 folds higher photocurrent than bare one, thereby exhibiting an excellent photo response. On comparison, Cu assisted SnO₂ nanostructured photo anode showcased improved performance and could serve as a potential photo anode for photovoltaic applications.

Keywords- SnO₂; Plasmon, FESEM; Field dependent dark and photoconductivity; UV-DRS

1. Introduction

Semiconductor metal oxides have been gaining extensive research interest in recent years, because of its wide band gap nature and diverse applications in various fields like gas sensors, solar cells, liquid crystal displays and photo catalytic dye degradation [1-3]. Among them, tin oxide (SnO₂), a wide band gap n-type semiconductor is a promising and multifunctional candidate which can be implemented in photovoltaic applications due to its attractive physical, chemical and optical properties [4]. The performance of solar cells especially Dye Sensitized Solar Cells (DSSCs) is largely limited by the inability to utilize visible region of solar spectrum and fast electron-hole recombination rate [5]. Doping noble metal (Plasmon) on SnO₂ is a promising way to improve its visible response. Metal nanoparticles support localized Surface Plasmon Resonance (SPR) which are collective oscillations of conduction electrons which strongly scatter the incident light near their resonances upon excitation [6]. In plasmonic metal/semiconductor hybrid nanostructures, a Schottky barrier exists at the junction interface between the metal and semiconductor. This barrier blocks the electron transfer from either way and thus it retards the recombination of electron-hole pairs [7]. Generally, Gold and Silver are employed as plasmons owing to their SPR wavelength in the visible regime. On the other hand, Copper (Cu) which is more abundant and less expensive than gold and silver and occurs with comparable absorbance in the visible region of the spectrum, is receiving attention as plasmon material recently [8]. Sol-gel technique is one of the optimal techniques to synthesize oxide nanomaterials as it provides good homogeneity, ease of controlling the doping level, requiring simple equipment and low-cost processing [9]. Thus in the present study, bare and plasmon (Cu) assisted SnO₂ nanoparticles were synthesized via sol-gel method and an investigation on structural, morphological and opto-electrical properties upon plasmon incorporation were done.

2. Materials and Methods

2.1 Synthesis Procedure

All the chemicals procured were of analytical grade reagents and used without further purification. Pure and plasmon supported SnO₂ nanoparticles were synthesized via sol-gel approach. In a typical synthesis process, an appropriate amount of stannous chloride was added to the mixture of isopropanol and deionized water taken in proportionate amounts. The resulting solution was constantly stirred for 24 h with drop wise addition of ammonia (until pH reaches 8). The obtained precipitate was then filtered, dried and calcined at 450°C for 4 hrs. Plasmon supported SnO₂ nanoparticles were synthesized in a similar manner, by adding 5 wt % of copper nitrate precursor into stannous chloride solution. The resultant product was light greenish and was further used for characterization techniques.

2.2 Characterizations

The crystal structure of the sample was identified by X-Ray Diffraction (XRD) analysis with Rigaku (Japan) X-ray diffractometer employing Cu K α radiation. The morphology was characterized using Field Emission Scanning Electron Microscopy (FESEM) with a SUPRA-55, Carl Zeiss, (Germany). The optical absorption properties of the sample were recorded using Perkin Elmer UV-Visible Diffuse Reflectance Spectrophotometer lambda 35 in the range of 200-800 nm. Surface areas were determined according to the Brunauett-Emmett-Teller (Micrometric ASAP 2020 Porosimeter) method. The field-dependent dark and photoconductivity studies were carried out using Keithley 6485 picoammeter.

3. Results and Discussion

3.1 Structural Analysis

Fig. 1 shows the XRD pattern of pure and plasmon assisted SnO₂ nanoparticles prepared through sol-gel technique. Both the samples confirmed the tetragonal structure of SnO₂ (JCPDS 041-1445) [4]. Characteristic peaks of Cu were not evident in Cu-SnO₂ sample and could be attributed to the incorporation of copper ions onto SnO₂ lattices [10]. The diffraction peaks at 26.6°, 33.9°, 38°, 51.8°, 54.8° and 64.7° correspond to (110), (101), (200), (211), (220) and (112) respectively in both cases. Employing Scherrer's formula, the average crystallite size of bare and doped samples was found to be 27 nm and 14 nm respectively [11]. Decreased crystallite size in the plasmonised sample is owing to smaller ionic radius of Cu²⁺ than Sn⁴⁺ and hence resulted in the contraction of lattice parameters [12].

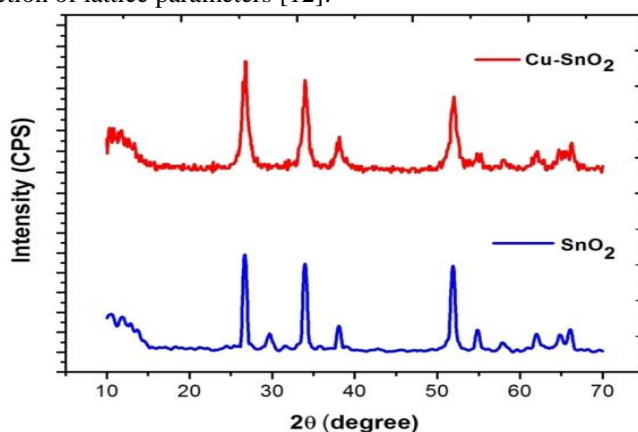


Fig 1. XRD patterns of pure and plasmon assisted SnO₂ nanoparticles

3.2 Morphological Analysis

FESEM analysis of bare and Cu assisted SnO₂ nanoparticles are shown in the Fig 2. It is observed from the micrographs, that the particles consist of large aggregates of spherical or rod shape which transform into smaller aggregates with doping leaving some pores in between. Compared to bare SnO₂, Cu doped SnO₂ samples possess decreased particle size of about 40 nm. Doping of Cu on SnO₂ has suppressed the growth of SnO₂ nanocrystallites thereby resulting in reduced particle size leading to superior surface area in the plasmonised sample [13].

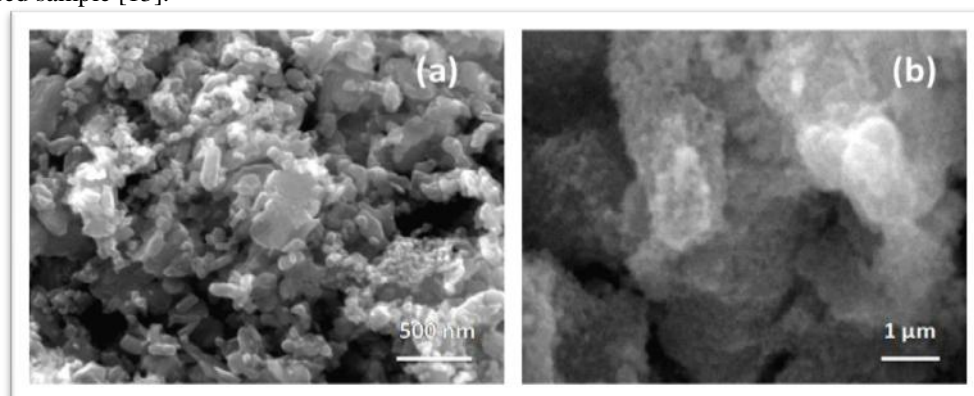


Fig 2. FESEM micrographs of pure and plasmon assisted SnO₂ nanoparticles

3.3 Optical Analysis

The optical absorbance of the samples was characterized using UV-DRS analysis and the images are given below. SnO₂ nanoparticles show an absorption peak at 310 nm which is almost near to the characteristic wavelength of SnO₂ nanoparticles [14]. In addition to the SnO₂ absorption peak occurring at around 300 nm (Blue shifted), the Cu doped samples explicitly shows another absorption peak towards visible region which supports the Surface Plasmon effect (SPR) of Cu nanoparticles. This phenomenon paves way for the plasmonised photoanode qualifying as a potential candidate for solar cell applications. The optical band gap energies were calculated with Kubelka – Munk (K-M) model [15]. From the K-M plot, the optical band gap value of bare and plasmonised SnO₂ nanoparticles was found to be 3.56 eV and 3.14 eV respectively. Reduction in the band gap energy of the plasmonised sample could be attributed to the charge-transfer transitions between the Copper ion - s electrons and the SnO₂ conduction or valence band [16].

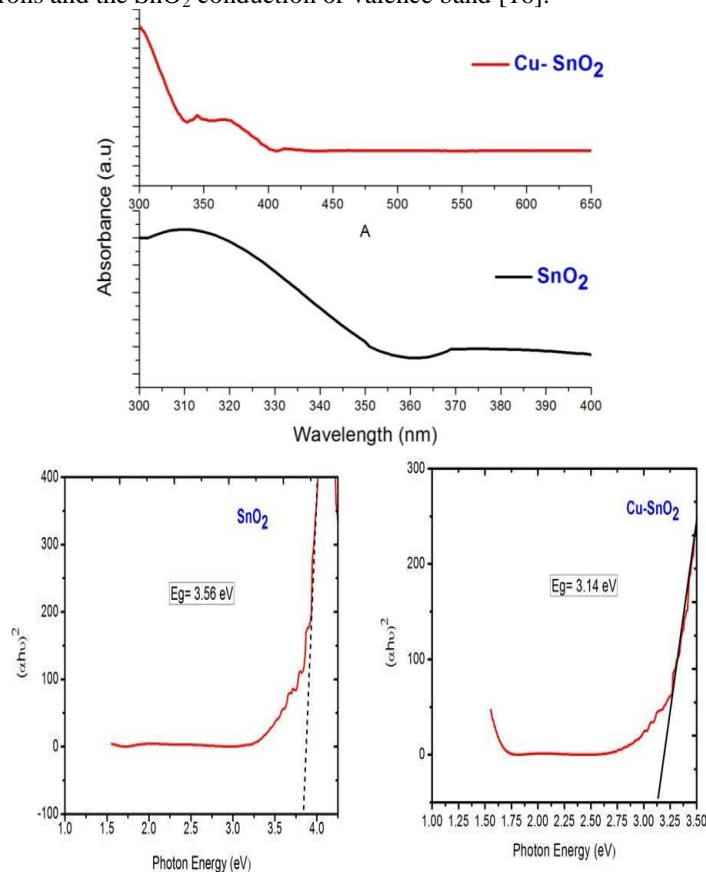


Fig 3. UV-DRS Spectra and Fig 4. K-M plots of pure and plasmon assisted SnO₂ nanoparticles

3.4 Electro-Optical Analysis

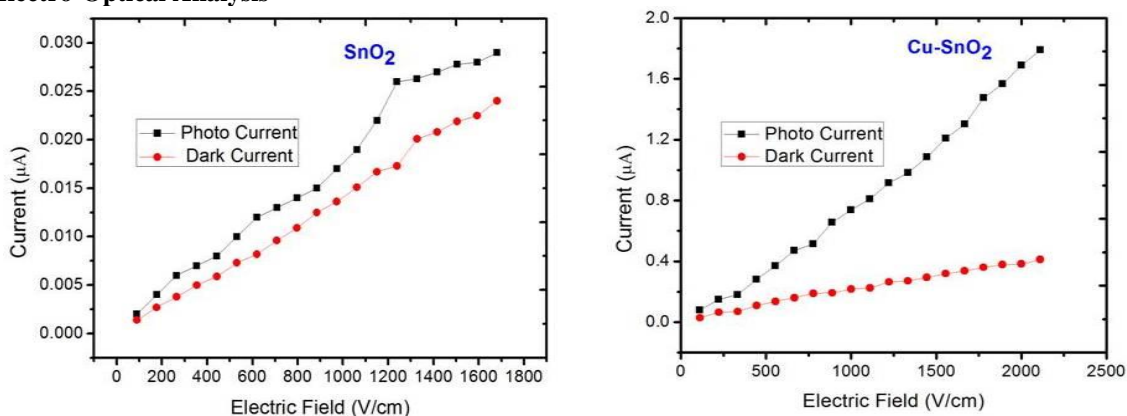


Fig 6. Field dependent dark and photocurrent plots of pure and plasmon assisted SnO₂ nanoparticles

Fig. 6 represents the field dependent dark and photoconductivity studies of bare and Cu assisted SnO₂ nanoparticles. Linear increase of currents with applied electric field is evidenced in both the samples depicting the ohmic nature of the contacts [17]. Compared to the bare, the plasmon enriched SnO₂ samples exhibited better photo response implying that on Cu doping, carrier concentration increases as well as surface conductivity enhances remarkably. For a fixed field of say 500 V/cm, the Cu supported sample shows increased dark and photo current of about 19 folds and 37 folds respectively compared to the pure SnO₂ nanoparticle presenting it as a prospective photoanode material for solar cell applications.

4. Conclusions

In summary, bare and Cu assisted SnO₂ nanoparticles are synthesized through facile sol-gel approach. XRD results confirmed the tetragonal crystal structure of the as-synthesized samples with reduced crystallite size in the case of plasmonised one. Decreased particle size in Cu supported SnO₂ nanoparticles led to an increased surface area which is beneficial for more dye absorption in DSSC applications. Better optical absorption was evidenced in plasmonised sample with slight shift towards visible region owing to surface plasmon resonance effect. Also, when compared to bare one, Cu supported sample possessed lesser band gap value and hence improved photoconducting behavior was witnessed in the latter. Thus a comparative investigation was made and based on the obtained results; we conclude that the Cu assisted SnO₂ nanoparticles exhibits superior structural, morphological and opto-electrical properties representing as a proficient photoanode for photovoltaic applications.

Acknowledgement

This work was funded by the Loyola College-Times of India Major Research Grants (6LCTOI14LIF002) and the authors acknowledge the same.

References

- [1]. Subramanian Mohan Priya, A. Geetha, K. Ramamurthi, J. Sol-Gel Sci Technol. (2016) DOI 10.1007/s10971-016-3966-7.
- [2]. Reddy AS, Figueiredo NM, Cavaleiro A, J Phys Chem Solids (2013) 74, 825.
- [3]. Tan L, Wang L, Wang Y, J Nano Mater. (2011) 10.
- [4]. S. S Mali, Chang Su Sim, Hyungjin Kim, Min Cheul Lee, Sangram D patil, Pramod S Patil, Chang Kook Hong J Nanopat Res (2015) 7 496.
- [5]. Wenguang Fan, Michael K. H. Leung, Molecules (2016) 27, 180.
- [6]. Arun Kumar Gupta, Pankaj Srivastava, Lal Bahadur, Appl. Phys. A., (2016) 122, 724.
- [7]. Wang X, Liow C, Bisht A, Liu X, Sum T C, Chen X, Li S, Adv. Mater. (2015) 27, 2207.
- [8]. F.Parveen et al. Solar Energy Materials & Solar Cells, (2016) 144, 371.
- [9]. H. Kose, A. O. Aydin, H. Akbulut, Acta Physica Polonica A, (2014) 125 345.
- [10]. M. A. Batal, G. Nashed, Fares Haj Jneed, J. Phys. Educ. (2012) 6, 2.
- [11]. V. Chandrakala et al, Acta Metall. Sin. (Engl. Lett.) (2016) DOI 10.1007/s40195-016-0409-y.
- [12]. Fang, L. M., Zu, X. T., Li, Z. J., Zhu, S., Liu, C. M., Zhou, W. L. et al., J Alloy Compd. (2008) 261, 454.
- [13]. S. Vadivel et al, J Mater Sci: Mater Electron, (2016) DOI 10.1007/s10854-015-3154-5.
- [14]. L. M. Fang, X. T. Zu, Z. J. Li, S. Zhu, C. M. Liu, L. M. Wang, , F. Gao, J. Mater. Sci: Mater. Electron. (2008) 19, 868.
- [15]. Kaustubh Basu et al. Scientific Reports (2016) 6 23312.
- [16]. P. Chetri, B. Saikia, A. Choudhury, J. Appl. Phys. (2013) 113, 233514.
- [17]. J. Merline Shyla et al, Int. J. Microstruct. Mater. Prop. (2013) 8, 6.